The 2009 IEEE/RSJ International Conference on
Intelligent Robots and Systems
October 11-15, 2009 St. Louis, USA

Estimation of Foot Orientation with Respect to Ground for an Above Knee Robotic Prosthesis

Glauco Garcia Scandaroli, Geovany Araújo Borges, João Yoshiyuki Ishihara,
Marco Henrique Terra, Adson Ferreira da Rocha, Francisco Assis de Oliveira Nascimento

Abstract— **This paper presents a new application in the field of rehabilitation robotics. It is part of a research project which consists of the development of a robotic leg prosthesis for above knee amputees. This application aims at providing real-time estimates of the prosthesis foot orientation with respect to ground. An Extended Kalman Filter (EKF) is used in order to estimate the foot orientation based on gyroscope and infrared measurements. Moreover a constraint equation is also included in the EKF to guarantee the constraints in the estimates. Preliminary tests were performed in a platform built for the prosthesis prototype. The results discussed in this paper reveal the feasibility of such technique.**

Index Terms— **above knee prosthesis, robotic prosthesis, non-linear estimation**

I. Introduction

THE LOSS of a limb can seriously worsen anyone's quality of life. Rehabilitation studies aim mainly at restoring lost motor function and supporting the treatment of motor disabilities caused by diseases or amputation. Prosthetics have been able to improve the mobility of lower limb amputees, but not yet to a level of complete satisfaction in the sense of comfort, energy consumption, stance phase stability, and gait symmetry. Most of today's commercially available lower limb prostheses are passive. Therefore their mechanical properties remain fixed independently of walking speed and terrain, consequently prostheses should be individually optimized for each patient.

The ability of a lower knee amputee to perform gait tasks better than an above knee amputee patient reflects the importance of the knee in locomotion [1]. In existing active above knee prosthesis the stiffness and damping at the prosthetic knee joint are applied by hydraulic, pneumatic [2]–[4] or magneto-rheological devices [5]–[7]. Clinical trials on commercially available prostheses, like Ottobock C-Leg and Össur Rheo, indicate that active prostheses offer advantages over mechanically passive designs [3], [8]. These advantages include enhanced smoothness of gait, decrease of metabolic rate, and decrease in hip work production. However current above knee prostheses do not worry about the foot control. Despite the development of active ankle-foot prostheses, above knee prostheses generally replaced the foot using a rubber ped mold or a carbon composite leaf-spring with no actuation in the ankle joint. Researchers have developed active ankle-foot prostheses that change stiffness and damping for distinct ground surfaces and walking speeds [7], [9]. In 1998, Klute *et al.* [10] were the first to build a powered ankle-foot prosthesis, which is based on pneumatic actuators known as McKibben muscles. Recently Au *et al.* [11] developed an active ankle-foot prosthesis that consists of a carbon composite foot coupled with a direct current motor, series and parallel springs. We observe in the literature that the available active prosthetic ankle-feet actuate in dorsiflexion and plantar flexion, but the eversion and invertion are neglected (see *e.g.* [9], [11], and references therein). The eversion and invertion movements are very important in stance phase and balance of human gait, which is corroborated in the research area of biped locomotion, as humanoid robots have the addition of this degree of actuation [12]–[14].

The purpose of this manuscript is to present an application that provides real-time estimates of the prosthesis foot orientation with respect to ground. We work in the context of an above knee robotic prosthesis prototype under development. The prototype has three degrees of actuation: one for the knee, which should aid the gait of the patient, and two for the ankle-foot in order to improve stability. One of ankle's degree of actuation refers to dorsiflexion and plantar flexion, while the other refers to eversion and invertion. The control of the prosthesis is in part based on surface electromyographic signal processing [15], and others, *e.g.* foot orientation with respect to ground, are used in order to increase reliability in the closed-loop system, since the prototype also possesses an active ankle-foot set. The surface electromyographic signals are responsible for providing the knee's movement intention, and the foot orientation are responsible for the ankle-foot set's movement. Currently, our effort concerns solving instrumentation, control and estimation problems. Further work will refer to increase prosthesis' adaption to human patients.

This paper focuses exclusively on the estimation of foot orientation with respect to ground, and the application is derived using gyroscope and infrared sensors, together with process and measurement models. The process model is based on the angular velocities taken from gyroscope sensors. The measurement is founded on distances from foot to ground given by infrared sensors. An Extended Kalman Filter is responsible for estimating such orientation and also the distance from foot to ground plan. A constraint equation

G. G. Scandaroli, G. A. Borges, and J. Y. Ishihara are with the Robotics, Automation and Vision Group (GRAV), Department of Electrical Engineering, University of Brasília, CP 4386, Brasília, DF, 70919-970, Brazil. (e-mails: glaucoscn@gmail.com, gaborges@ene.unb.br, ishihara@ene.unb.br).

M. H. Terra is with University of São Paulo at São Carlos, CP 359, São Carlos, SP, 13566-590, Brazil. (e-mail: terra@sel.eesc.usp.br).

A. F. da Rocha and F. A. O. Nascimento are with the Digital Signal Processing Group (GPDS), Department of Electrical Engineering, University of Brasília, CP 4386, Brasília, DF, 70919-970, Brazil. (e-mails: adson@ene.unb.br, assis@ene.unb.br).

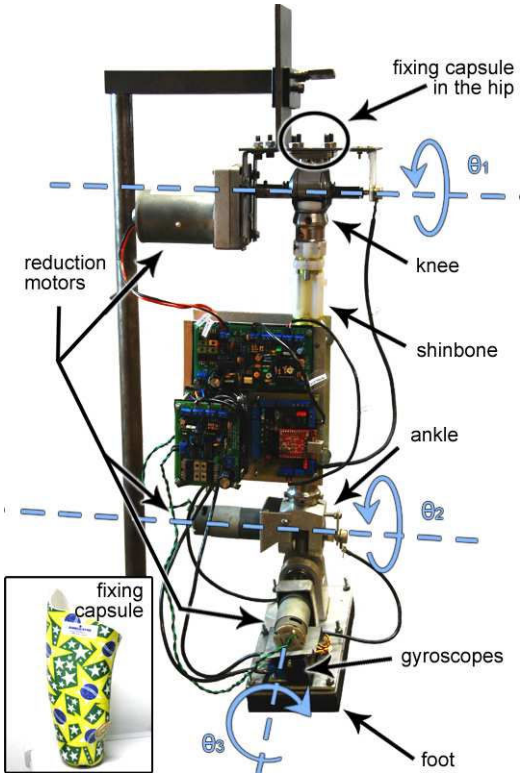

Fig. 1. Picture of the prosthesis under development

was included in the EKF in order to keep the coherence of estimates. Up to the author's knowledge, there is no similar work reported in the literature. A solution to this problem would allow the use of the prosthesis prototype for natural terrain walking, where foot positioning with respect to ground should be controlled. Due to project's stage tests were performed in the plataform used for the prosthesis' development instead of clinical trials.

This paper is organized as follows. In Section II there is a brief description of the prosthesis prototype currently under development. Section III presents the foot orientation variables and how sensors cope in the estimation of these variables. In Section IV there is a short review of the Extended Kalman filter and estimation with state constraints, followed by the state equations used in the estimation process. Section V presents the estimation results of the prosthesis foot orientation, followed by conclusions concerning the estimation as well as the ongoing development in the context of this project in Section VI.

II. Prosthesis prototype description

Fig. 1 shows a picture of the robotic prosthesis prototype under development. It is based on an originally passive Ottobock 3R15 knee model, and after some adaptions the prototype has three degrees of actuation: one for the knee (sagittal plane), and two for the ankle (sagittal and frontal plane). The actuation on the knee joint aims at aiding the gait of the patient, and ankle actuation is addressed to improve stability. The three degrees of freedom are associated to

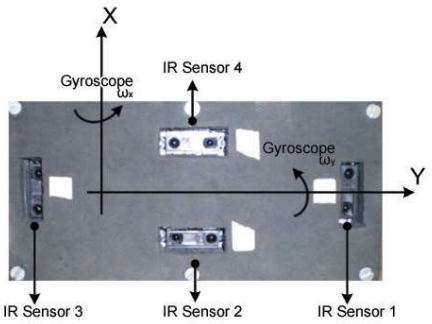

Fig. 2. Infrared sensors placement underneath the foot, and gyroscopes velocities measurement orientation

angles θ_1, θ_2, θ_3, and each joint is controlled by a direct current motor and a switched current source actuator. The choice of electrical motors is due to the fact that fast high torque, very efficient motors and batteries are currently available in relatively small packages. This prototype will fixed to the patient's upper leg through a fixing capsule, containing the surface electromyographic signals measurement module. Currently the prosthesis is attached to a plataform built specially to aid the assembly of electronic circuitry and likewise for experimentation.

Concerning the foot instrumentation, it is equipped with two Analog Devices ADXRS300 gyroscopes, and four Sharp GP2D120 distance measuring infrared sensors mounted underneath the foot (Fig. 2). These infrared sensors where chosen due to the low influence on the color of reflective objects, thus the ground color need not to be calibrated, and also of reflecting conditions in the measured distance according to the manufacturer, ranges from 18% to 90% of reflectivity. The infrared sensors can detect objects placed from 4 *cm* up to 30 *cm*. There are no foot pad pressure sensors yet on the prototype, though when gait experimets occur we will probably have to consider that. A 32-bit ARM7 core based AT91SAM7S64 microcontroller from ATMEL® is responsible for controlling the joints, gathering data from the sensors and communicating with the computer through a RS-485 serial bus. The six analog sensors (two gyroscopes and four infrared sensors) are connected to a 10-bit ADC. There are also three resistive potentiometers connected to the three joints such that relative angle between femur, shinbone and ankle can be directly measured. Each potentiometer is connected to a channel of the ADC. All sensor data is gathered at 10 *ms* sampling period. The prosthesis foot orientation is currently estimated at a PC with the data provided by the microcontroller. Prior experimentation on patients occurs, the estimator will be embedded into the microcontroller.

III. Prosthesis foot orientation variables and sensing modelling

In order to describe the orientation of the foot with respect to ground, denote by $X \times Y \times Z$ the reference cartesian system as depicted in Fig. 3. In this figure, $X \times Y$ is the foot plan, and Ξ represents the ground plan. Prosthesis foot orientation

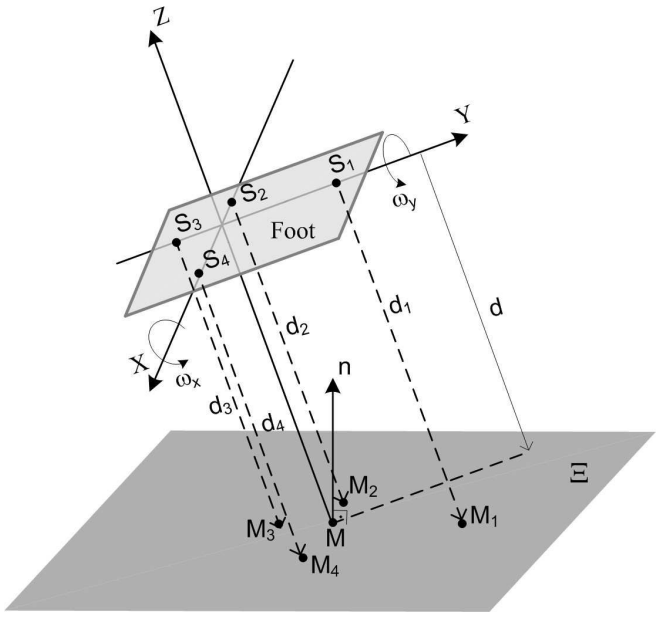

Fig. 3. Foot orientation with respect to ground and sensor measurements

with respect to ground is described by $\mathbf{n} = \begin{bmatrix} n_x & n_y & n_z \end{bmatrix}^T$, the unit length normal vector to Ξ described in the reference system $X \times Y \times Z$, and d is the distance in Z axis of the ground plan to the origin of $X \times Y \times Z$.

S_1, S_2, S_3 and S_4 are the positions of the infrared sensors in foot plan. It is considered that such sensors make measurements perpendicular to $X \times Y$ plan in the direction of Ξ. Such measurements are taken in points M_1, M_2, M_3 and M_4, and denoted d_j, $j = 1,\ldots,4$, all of them with the same variance σ_d^2, meaning that infrared sensors have the same uncertainty level. The coordinates $\mathbf{m}_j$ in $X \times Y \times Z$ of $M_j \in \Xi$ are given by

$$\mathbf{m}_j = \mathbf{s}_j + \begin{bmatrix} 0 \\ 0 \\ -d_j \end{bmatrix} = \begin{bmatrix} s_{j,x} \\ s_{j,y} \\ -d_j \end{bmatrix}. \tag{1}$$

where $\mathbf{s}_j = \begin{bmatrix} s_{j,x} & s_{j,y} & 0 \end{bmatrix}^T$ are the coordinates of S_j corresponding to the placement of the j-th infrared sensor. Since $M \in \Xi$, with coordinates $\mathbf{m} = \begin{bmatrix} 0 & 0 & -d \end{bmatrix}^T$, one has

$$\mathbf{n}^T(\mathbf{m}_j - \mathbf{m}) = 0$$

for each infrared sensor measurement, resulting in

$$d_j = \frac{dn_z + s_{j,y}n_y + s_{j,x}n_x}{n_z} \tag{2}$$

as equation relating the jth sensor distance measurement d_j to foot orientation variables $\mathbf{n}$ and d.

The two gyroscopes provide angular motion measurements of the foot in X and Y axis. Such measurements are angular velocities ω_x and ω_y as shown in Fig. 3, and take effect in $\mathbf{n}$ according to

$$\dot{\mathbf{n}} = \frac{\partial \mathbf{n}}{\partial \phi_x}\omega_x + \frac{\partial \mathbf{n}}{\partial \phi_y}\omega_y$$

where $\omega_x = \frac{d\phi_x}{dt}$ and $\omega_y = \frac{d\phi_y}{dt}$ with ϕ_x and ϕ_y being small rotation angles in axis X and Y, respectively. The partial derivatives are evaluated as

$$\begin{aligned} \frac{\partial \mathbf{n}}{\partial \phi_x} &= \lim_{\Delta\phi_x \longrightarrow 0} \frac{\Delta \mathbf{n}}{\Delta \phi_x} = \lim_{\Delta\phi_x \longrightarrow 0} \frac{\mathbf{R}_X(\Delta\phi_x)\mathbf{n} - \mathbf{n}}{\Delta\phi_x} \\ \frac{\partial \mathbf{n}}{\partial \phi_y} &= \lim_{\Delta\phi_y \longrightarrow 0} \frac{\Delta \mathbf{n}}{\Delta \phi_y} = \lim_{\Delta\phi_y \longrightarrow 0} \frac{\mathbf{R}_Y(\Delta\phi_y)\mathbf{n} - \mathbf{n}}{\Delta\phi_y} \end{aligned}$$

with

$$\mathbf{R}_X(\theta) = \begin{bmatrix} 1 & 0 & 0 \\ 0 & \cos(\theta) & \sin(\theta) \\ 0 & -\sin(\theta) & \cos(\theta) \end{bmatrix},$$

$$\mathbf{R}_Y(\theta) = \begin{bmatrix} \cos(\theta) & 0 & -\sin(\theta) \\ 0 & 1 & 0 \\ \sin(\theta) & 0 & \cos(\theta) \end{bmatrix}$$

being the basic rotations of angle θ about X and Y axis, respectively. Further development results in

$$\dot{\mathbf{n}} = \begin{bmatrix} -n_z\omega_y \\ n_z\omega_x \\ -n_y\omega_x + n_x\omega_y \end{bmatrix}. \tag{3}$$

It should be pointed out that the angular velocity about Z axis is considered small when compared to ω_x and ω_y. This is usually the case for general movement of foot from this section.

IV. Prosthesis foot orientation estimation

A. Extended Kalman filter and constrained estimation

This section reviews nonlinear state estimation via the Extended Kalman filter (EKF) and constrained estimation. Notations on EKF are taken from [16].

Consider the following nonlinear discrete time system:

$$\mathbf{x}_{k+1} = \mathbf{f}_k(\mathbf{x}_k, \mathbf{u}_k) + \mathbf{w}_k \tag{4}$$

$$\mathbf{z}_k = \mathbf{h}_k(\mathbf{x}_k) + \mathbf{v}_k \tag{5}$$

where k is the time index, $\mathbf{x} \in \Re^n$ is the state vector, $\mathbf{u} \in \Re^m$ is the known control input, $\mathbf{z} \in \Re^p$ is the measurement, $\mathbf{f}_k : (\Re^n, \Re^m) \rightarrow \Re^n$ and $\mathbf{h}_k : \Re^n \rightarrow \Re^p$ are nonlinear process and measurement functions, $\mathbf{w}_k \in \Re^n$ and $\mathbf{v}_k \in \Re^m$ are noise inputs. $\mathbf{v}_k$ and $\mathbf{w}_k$ are zero mean uncorrelated white gaussian processes, $\mathbf{x}_0$ is a gaussian random variable vector with known covariance $\mathbf{P}_0$. We assume that $\mathbf{w}_k$, $\mathbf{v}_k$ and $\mathbf{x}_0$ are mutually independent, $E[\mathbf{w}_k\mathbf{w}_j^T] = \mathbf{Q}_k\delta_{kj}$, $E[\mathbf{v}_k\mathbf{v}_j^T] = \mathbf{R}_k\delta_{kj}$ where δ_{kj} is the Kronecker delta function (*i.e.* $\delta_{kj} = 1$ if $k = j$, 0 otherwise), and $\mathbf{x}_0 \sim N(\bar{\mathbf{x}}_0, \mathbf{P}_0)$. $\mathbf{R}_k$, $\mathbf{Q}_k$ and $\mathbf{P}_0$ are positive semidefinite covariance matrices. We denote:

$$\mathbf{F}_k = \left.\frac{\partial \mathbf{f}_k(\mathbf{x})}{\partial \mathbf{x}}\right|_{\mathbf{x}=\hat{\mathbf{x}}_{k|k}}, \qquad \mathbf{H}_k = \left.\frac{\partial \mathbf{h}_k(\mathbf{x})}{\partial \mathbf{x}}\right|_{\mathbf{x}=\hat{\mathbf{x}}_{k|k-1}} \tag{6}$$

The EKF based estimation process can be split into two steps: prediction and correction. The equations are as

follows:

$$\hat{\mathbf{x}}_{k|k-1} = \mathbf{f}_k(\hat{\mathbf{x}}_{k-1|k-1}, \mathbf{u}_k) \quad (7)$$

$$\boldsymbol{\Sigma}_{k|k-1} = \mathbf{F}_k \boldsymbol{\Sigma}_{k-1|k-1} \mathbf{F}_k^T + \mathbf{Q}_k \quad (8)$$

$$\mathbf{K}_k = \boldsymbol{\Sigma}_{k|k-1} \mathbf{H}_k^T (\mathbf{H}_k \boldsymbol{\Sigma}_{k|k-1} \mathbf{H}_k^T + \mathbf{R}_k)^{-1} \quad (9)$$

$$\hat{\mathbf{x}}_{k|k} = \hat{\mathbf{x}}_{k|k-1} + \mathbf{K}_k \left(\mathbf{z}_k - \mathbf{h}_k(\hat{\mathbf{x}}_{k|k-1})\right) \quad (10)$$

$$\boldsymbol{\Sigma}_{k|k} = (\mathbf{I} - \mathbf{K}_k \mathbf{H}_k) \boldsymbol{\Sigma}_{k|k-1} \quad (11)$$

where (7)-(8) are EKF's prediction step, and (9)-(11) the correction step. Filter initialization is provided by $\boldsymbol{\Sigma}_{0|0} = \mathbf{P}_0$, $\hat{\mathbf{x}}_{0|0} = \bar{\mathbf{x}}_0$.

There is often known information that does not fit into the Kalman filter equations. For instance, when we know that the states satisfy some equality constraint $\mathbf{g}(\mathbf{x}) = \mathbf{c}$, where $\mathbf{c} \in \Re^r$ is a known vector, and $\mathbf{g} : \Re^n \to \Re^r$ is a nonlinear constraint function. One way to consider the state constraint in the estimation process consists in augmenting the measurement equation (5) with perfect measurements of the state vector:

$$\begin{bmatrix} \mathbf{z}_k \\ \mathbf{c} \end{bmatrix} = \begin{bmatrix} \mathbf{h}_k(\mathbf{x}_k) \\ \mathbf{g}(\mathbf{x}_k) \end{bmatrix} + \begin{bmatrix} \mathbf{v}_k \\ \mathbf{0} \end{bmatrix} \quad (12)$$

hence EKF correction step (9)-(11) is evaluated by replacing the measurement equation (5) by the augmentation (12). The interested reader can consult, for instance, [17].

B. System modelling

Let $\mathbf{x}_k = \begin{bmatrix} \mathbf{n}_k^T & d_k \end{bmatrix}^T = \begin{bmatrix} n_{x,k} & n_{y,k} & n_{z,k} & d_k \end{bmatrix}^T$ the system state variable corresponding to foot orientation at discrete time k, and let $\mathbf{u}_k = \begin{bmatrix} \omega_{x,k} & \omega_{y,k} \end{bmatrix}^T$ the gyroscopes measurements at discrete time k. The following model describes the evolution of state variables between measurements:

$$\mathbf{x}_{k+1} = \mathbf{f}(\mathbf{x}_k, \mathbf{u}_k) + \mathbf{w}_k \quad (13)$$

$$= \begin{pmatrix} n_{x,k} - T n_{z,k} \omega_{y,k} \\ n_{y,k} + T n_{z,k} \omega_{x,k} \\ n_{z,k} - T n_{y,k} \omega_{x,k} + T n_{x,k} \omega_{y,k} \\ d_k \end{pmatrix} + \mathbf{w}_k \quad (14)$$

In above, concerning evolution of the normal vector $\mathbf{n}_k$, Eq. (3) has been used in a first order Euler approximation with sampling period T. $\mathbf{w}_k$ is a Gaussian random noise encompassing gyroscope uncertainty as well as neglecting rotation about Z axis. Further, it has been considered a random evolution for d_k with Gaussian distribution, represented by the last entry of $\mathbf{w}_k$. It should be pointed out that (14) does not guarantee $\mathbf{n}_{k+1}$ with unit length. Thus, the following constraint should be considered:

$$g(\mathbf{x}_k) = n_{x,k}^2 + n_{y,k}^2 + n_{z,k}^2 = 1. \quad (15)$$

According to (2), a set $\mathbf{z}_k = \begin{bmatrix} d_{1,i} & d_{2,i} & d_{3,i} & d_{4,i} \end{bmatrix}^T$ of measurements from infrared sensors are related to system state as

$$\mathbf{z}_k = \mathbf{h}_k(\mathbf{x}_k) + \mathbf{v}_k \quad (16)$$

$$= \begin{pmatrix} \frac{d_k n_{z,k} + s_{1,y} n_{y,k} + s_{1,x} n_{x,k}}{n_{z,k}} \\ \frac{d_k n_{z,k} + s_{2,y} n_{y,k} + s_{2,x} n_{x,k}}{n_{z,k}} \\ \frac{d_k n_{z,k} + s_{3,y} n_{y,k} + s_{3,x} n_{x,k}}{n_{z,k}} \\ \frac{d_k n_{z,k} + s_{4,y} n_{y,k} + s_{4,x} n_{x,k}}{n_{z,k}} \end{pmatrix} + v_k \quad (17)$$

with $\mathbf{v}_k \sim N(\mathbf{0}, \sigma_d^2 \mathbf{I}_4)$ being the measurement noise. The above equation corresponds to a non-linear measurement model. It considers all infrared sensor measurements have the same uncertainty level, represented by variance σ_d^2, this has been verified in practice. Rewritting the measurement model (17) in order to include the constraint (15) results in

$$\begin{bmatrix} \mathbf{z}_k \\ 1 \end{bmatrix} = \begin{bmatrix} \mathbf{h}_k(\mathbf{x}_k) \\ g(\mathbf{x}_k) \end{bmatrix} + \begin{bmatrix} \mathbf{v}_k \\ 0 \end{bmatrix} \quad (18)$$

thus at each sampling step k, gyroscope measurements are used in EKF's prediction step (7)-(8) with process model (14). Infrared sensors are used in EKF's correction step (9)-(11) with the augmented measurement-constraint equation (18).

It is possible to initialize parameter $\mathbf{x}_0$ by gathering a single measurement $\mathbf{z}_0$, and solving Eqs. (17) and (15) using nonlinear optimization. One may argue that, instead of using the EKF approach, only the nonlinear optimization could be evaluated at each sampling step. Nevertheless, this optimization cannot be solved at the proposed 10 *ms* sampling step using such a 32-bit ARM7 microcontroller. Additionally, information given by the process model would not be considered, thus weakening the whole solution.

V. Experimental results

In this section, an experimental evaluation of the proposed foot orientation estimator is presented. The prosthesis shinbone was set up in a perpendicular position with respect to floor and several control signals were sent to the motors responsible for rotation in X and Y axis. Gyroscope and infrared measurements were gathered in real-time during 35 *s* at $T = 10$ *ms* sampling period. Further, a potentiometer installed at foot provided direct angular measurements in X axis, which is used to evaluate the performance in estimating the n_x normal vector component. This sensor can be used to partially validate the results of the proposed filter by giving a ground truth reference for n_x. However, the potentiometer measurements cannot be used in replacement of the proposed system because its measurement is taken with respect to the prosthesis shinbone, not with respect to ground. Thich is not the case with the prosthesis installed in a human patient.

In this experimentation, without loss of generality, the foot is considered initially parallel with respect to ground, but with large uncertainty on vector $\mathbf{n}$ actual value. Thus EKF was initialized with parameters $\bar{\mathbf{x}}_0$ and $\mathbf{P}_0$ as follows

$$\bar{\mathbf{x}}_\mathbf{0} = \begin{bmatrix} 0 & 0 & 1 & 7 \end{bmatrix}^T \quad (19)$$

$$\mathbf{P}_0 = \mathrm{diag}\left(\begin{bmatrix} \frac{1}{9} & \frac{1}{9} & \frac{1}{9} & 15 \end{bmatrix}\right). \quad (20)$$

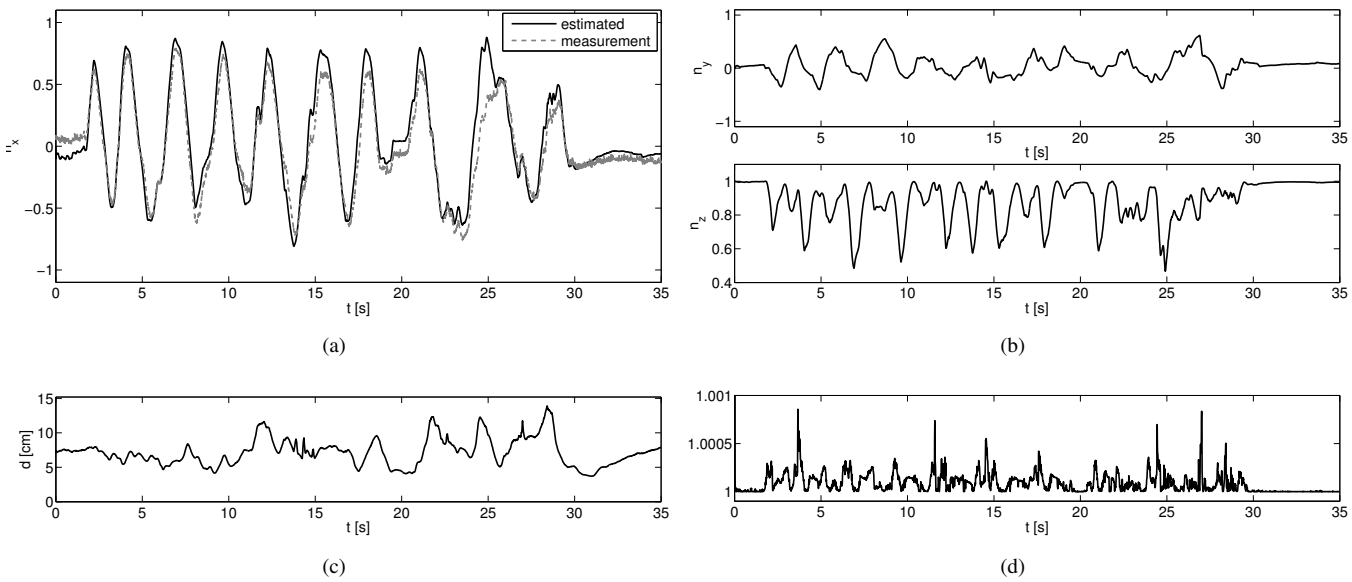

Fig. 4. (a) Vector $\mathbf{n}$ component n_x estimated (solid black) and measured (dashed gray); (b) vector $\mathbf{n}$ components n_y, n_z estimated; (c) Distance d of foot to ground plan estimated; (d) norm of vector $\mathbf{n}$ (right plot).

It can be seen that the initial state $\bar{\mathbf{x}}_0$ is a solution of constraint (15). $\bar{\mathbf{x}}_0$ corresponds to the foot being parallel to ground and at a distance of approximately 7 *cm*. The covariance matrix $\mathbf{P}_0$ has elements large enough, so that $\bar{\mathbf{x}}_0$ is be quickly forgotten with the arrival of measurements $\mathbf{z}_k$. This choice makes the estimator robust to the initial condition's lack of knowledge. Matrices $\mathbf{Q}_k$ and $\mathbf{R}_k$ were chosen based on sensors' specifications, and considering that the evolution of distance from foot to ground d is completely unknown. The parameters $\mathbf{Q}_k$ and $\mathbf{R}_k$ were set as follows:

$$\mathbf{Q}_k = \text{diag}\left(\begin{bmatrix} 10^{-8} & 10^{-8} & 10^{-8} & 10^{-4} \end{bmatrix}\right) \quad (21)$$

$$\mathbf{R}_k = \text{diag}\left(\begin{bmatrix} 0.1^2 & 0.1^2 & 0.1^2 & 0.1^2 \end{bmatrix}\right) \quad (22)$$

the estimated orientation variables and the norm of vector $\mathbf{n}$ are presented in Fig. 4.

Fig. 4(a) presents the estimated n_x and the corresponding measured projection based on potentiometer readings. It can be seen that the estimated n_x component is very close to that measured by the potentiometer throughout the whole experiment. A small difference at 25 *s* is possibly caused by an instantaneous error in gyroscopes' measurement that could not be completely corrected by the estimator. At approximately 27 *s* it can be seen that the estimated component n_x returns to be close to the potentiometer's value, and thus continues until the end of the experiment, meaning that the estimator can fetch up the orientation variables even having short duration prediction problems. Fig. 4(b) illustrates the results on components n_y, and n_z. For these estimates there are no ground truth measurements for comparison. Fig. 4(c) presents the distance d from foot to ground plan. Just as what happened with components n_y and n_z there is no ground truth measurement for comparison. However, it can be seen that d is approximately 7 *cm* in experiment's begin and end. This means that when the EKF estimates an orientation parallel with respect to ground, the distance d is estimated with the same value. This is an interesting result, whereas during this experimentation the shinbone was not moved, hence for the same foot orientation one must obtain the same distance d. Fig. 4(d) presents the norm of vector n throughout the experiment. One can see that vector $\mathbf{n}$ has norm very close to unity throughout the experiment with errors lower then 0.01%, although the measurement-constraint function (12) is linearized at the predicted state $\hat{\mathbf{x}}_{k|k-1}$.

Fig. 5. Prosthesis foot orientation estimator providing estimates to a controller responsible for keeping foot parallel with respect to ground.

Despite the fact that the joint control is not part of this work, the proposed system is currently used to provide foot orientation estimates to a controller responsible for keeping the foot parallel with respect to ground, Fig. 5 shows a situation where both the estimator and the controller are working. For those interested, videos of the project are available at: `http://www.ene.unb.br/~gaborges/reabilitacao_protese/index_en.htm`.

VI. Conclusions, ongoing work

This article presented an application which provides real-time estimates of the prosthesis foot orientation with respect to ground. The foot orientation variables and their relation to sensors' measurements were presented. An Extended Kalman filter with constrained states was used in order to estimate the orientation variables. Satisfactory results have shown that the prosthesis foot orientation can be estimated with this procedure. Regardless of EKF being a linearized estimator, it is presented robust enough to recover from prediction errors. Results on distance estimation appeared to be consistent, although there is no way to compare the estimated distance with the real one.

There is still room for improvement, mainly for considering an evolution model for the distance between foot and ground considering the prosthesis' movement. In order to reduce the sensitivity to measurement errors, such as masked off sensors, it should be included a statistical test (such as the mahalanobis test) for each infrared sensor, in order to detect and then ignore such mistaken measurement. Current work refers to intention estimation from surface electromyographic signal processing [15]. Future work will address the integration of knee's movement intention and the movement of the ankle-foot set.

VII. Acknowledgments

G. G. Scandaroli is supported by a grant from CAPES, and was partially funded by FAP-DF. G. A. Borges, J. Y. Ishihara, M. H. Terra, and A. F. da Rocha are partially supported by research grants from CNPq. The authors appreciate Davi Anders Brasil for developing the foot's instrumentation system.

References

[1] C. T. Huang, J. R. Jackson, and N. B. Moore, "Amputation: energy cost of ambulation," *Arch. Phys. Med. Rehabil.*, vol. 60, pp. 18–23, 1979.

[2] S. Zahedi, "The results of the field trail of the ENDOLITE intelligent prosthesis," in *Proceedings XII International Congress INTERBOR*, 1993.

[3] J. Kastner, R. Nimmervoll, and I. P. Wagner, "What are the benefits of the Otto Bock C-leg? a comparative gait analysis of C-leg, 3R45 and 3R80," *Med. Orthop. Tech*, vol. 119, pp. 131–137, 1999.

[4] D. Zlatnik, B. Steiner, and G. Schweitzer, "Finite-state control of a trans-femoral (TF) prosthesis," *IEEE Transactions on Control Systems Technology*, vol. 10, no. 3, pp. 408–420, 2002.

[5] J.-H. Kim and J.-H. Oh, "Development of an above knee prosthesis using MR damper and leg simulator," in *Proceedings 2001 IEEE International Conference on Robotics & Automation*, Seoul, Korea, 2001, pp. 3686–3691.

[6] H. Herr and A. Wilkenfeld, "User-adaptive control of a magnetorheological prosthetic knee," *Industrial Robot: An International Journal*, vol. 30, no. 1, pp. 42–55, 2003.

[7] Össur, Inc. [On-line] 2009, http://www.ossur.com.

[8] J. L. Johansson, D. M. Sherrill, P. O. Riley, B. Paolo, and H. Herr, "A clinical comparison of variable-damping and mechanically passive prosthetic knee devices," *American Journal of Physical Medicine & Rehabilitation*, vol. 84, pp. 563–575, 2005.

[9] C. Li, M. Tokuda, J. Furusho, K. Koyanagi, S. Morimoto, Y. Hashimoto, A. Nakagawa, and Y. Akazawa, "Research and development of the intelligently–controlled prosthetic ankle joint," in *Proceedings of the 2006 IEEE International Conference on Mechatronics and Automation*, June 2006, pp. 1114–1119.

[10] G. Klute, J. Czerniecki, and B. Hannaford, "Development of powered prosthetic lower limb," in *Proceedings of the 1st National Mtg, Veterans Affairs Rehab*, Washington, DC, October 1998.

[11] S. K. Au, J. Weber, and H. Herr, "Powered ankle–foot prosthesis improves walking metabolic economy," *IEEE Transactions on Robotics*, vol. 25, no. 1, pp. 51–66, Feb. 2009.

[12] K. Hirai, M. Hirose, Y. Haikawa, and T. Takenaka, "The development of Honda humanoid robot," in *Proceedings of IEEE International Conference on Robotics and Automation*, vol. 2, May 1998, pp. 1321–1326.

[13] Y. Sakagami, R. Watanabe, C. Aoyama, S. Matsunaga, N. Higaki, and K. Fujimura, "The intelligent ASIMO: system overview and integration," in *IEEE International Conference on Intelligent Robots and System, 2002*, vol. 3, 2002, pp. 2478–2483.

[14] I.-W. Park, J.-Y. Kim, J. Lee, and J.-H. Oh, "Mechanical design of humanoid robot platform KHR-3 (KAIST humanoid robot 3: HUBO)," in *5th IEEE-RAS International Conference on Humanoid Robots*, Dec. 2005, pp. 321–326.

[15] A. Delis, J. Carvalho, A. da Rocha, F. Nascimento, and G. Borges, "Development of a myoelectric controller based on knee angle estimation," in *Proceedings 2nd International Conference on Biomedical Electronics and Devices*, 2009, pp. 97–103.

[16] B. D. O. Anderson and J. B. Moore, *Optimal Filtering*. Dover Publications, 2005.

[17] D. Simon, *Optimal State Estimation*. Wiley & Sons, 2006.